Investigation of Narrowband Interference Filtering Algorithms for Galileo CBOC Signals

ALEXANDRU RUSU-CASANDRA
Department of Telecommunications
Politehnica University of Bucharest
Bucharest, ROMANIA
rusu.alex[at]yahoo[dot]com

ELENA-SIMONA LOHAN
Department of Communications Engineering
Tampere University of Technology
Tampere, FINLAND
elena-simona.lohan@tut.fi

GONZALO SECO-GRANADOS
Department of Telecommunications and System Engineering
Universitat Autonoma de Barcelona
Barcelona, SPAIN
gonzalo.seco@uab.es

ION MARGHESCU
Department of Telecommunications
Politehnica University of Bucharest
Bucharest, Romania
marion@comm.pub.ro

Abstract: - Global Navigation Satellite Systems (GNSS) systems share the same spectrum with other telecommunication systems. Papers based on actual RF measurement campaigns have reported that loss-of-lock on the navigational signals can happen to unaided GNSS receivers near radio and TV broadcast transmitters [5]. Radionavigation and communication systems can generate interference to GNSS receivers close to airports. Thus it is important to optimize the solutions against interferences. In this paper, we propose an innovative approach, because we address the particular issue of filtering the Continuous Wave Interferences (CWIs) affecting Multiplexed-Binary-Offset-Carrier (MBOC) Galileo navigation signal, using several filtering techniques. This comparative study is novel in the GNSS literature, to the best of the authors' knowledge.

Key-words: - GNSS, Continuous Wave Interference, Multiplexed Binary Offset Carrier, notch filter

1 Introduction

Presently, GNSS systems like European Union's Galileo operate in the the IEEE L frequency band, which is located approximately from 1 to 2 GHz. [1]. Other telecommunication systems that share the L band are enumerated next [2]: aeronautical navigation systems like civilian Distance Measuring Equipment (DME); air traffic control radars; military and government systems for terrestrial communication, navigation and identification; amateur radio communications; telemetry and telecommand services for aircraft and missiles; Digital Audio Broadcast; mobile satellite communication systems like Inmarsat and Iridium. It can be observed that the spectrum around the GNSS frequency bands is heavily used and thus unintentional Radio Frequency (RF) interference is likely to occur for a GNSS receiver at a low level. Naturally, also deliberate jamming of the GNSS signals can happen.

The topic of narrowband filtering has been investigated e.g. in [13-15]. In [13, 15], notch filters are used for the detection and filtering of narrowband CWI in GNSS signals. In this paper we present three techniques that are adaptive and can detect and filter an unlimited number of CWIs. To study the effectiveness of each method, we compare

ISBN: 978-1-61804-138-8

the tracking Root Mean Square Error (RMSE) curves versus Signal-to-Interference Ratios (SIRs), at different Carrier-to-Noise densities (C/N_0s). The second section of this work presents the potential RF interferences in GNSS. The next section discusses the properties of the Binary-Offset-Carrier (BOC) modulation. CWI filtering algorithms are presented in the next Section and the simulation setup is described in section 5. The results obtained from the Matlab simulations are illustrated in section 6 and the conclusions are presented in the last section.

2 RF Interferences in GNSS

RF interferences can be categorized after the size of the frequency spectrum occupied by the interference signal, relative to the size of the bandwidth used by GNSS signal, in wideband or narrowband. A single frequency sine wave (Dirac impulse), called a CWI is the most limited narrowband interference. Narrowband interferences can be produced by the overflow of energy from neighboring bands, situated above or below one of the GNSS carrier frequencies, by harmonics, or by intermodulation products [2]. Harmonics are signals with frequencies representing integer multiples of the carrier frequency of an emitter and are generated by nonlinearities upon transmission. Intermodulation products can be produced when signals of different frequencies are applied through a nonlinear device.

Aeronautical navigation is one of the main applications of GNSS for civilian purposes, because GNSS can optimize the efficient management of the airspace, can enhance air traffic safety and can lower air traffic costs. For this, GNSS services must provide [3]: accuracy, integrity, continuity and global availability. To improve the integrity of the navigation service, Galileo is planning to provide a Safety of Life (SoL) service in the E5a and E5b subbands of the L band. The service will deliver to the user a timely warning of a malfunctioning system status.

In the last decades, DME employed the E5 subband. Fortunately this system is transmitting very short pulses (3.6μs), but the transmission power reaches high values, up to 2 kW, compared to the transmitting power of approximate 100 W from a navigation satellite. There is also a major difference between the distances from these emitters to the receiver: a GNSS receiver aboard an aircraft can be as close as 0.1 km from an emitting DME station, but it will always be about 23200 km away from the emitter onboard the GNSS satellite. Thus it can be said that the reception of a GNSS signal can get very bad while a DME station is emitting its pulse signal. One technique of mitigating this interference between the DME and the Galileo receiver is the ''pulse blanking method" [9]. With this technique the receiver input is switched off when a pulse is detected. The degradation of the positioning accuracy is not strong because the duration of the pulse is quite short. However, in the situations when signals from several DME stations are received, or when the air traffic is busy and numerous pulses are emitted, they become very frequent and the receiver must cut off the input often. As a result, the receiver will not be able to properly acquire and track the signal, because it lacks many samples [4].

3 BOC modulation and tracking

BOC modulation is a spread-spectrum modulation method that is presently utilized in Galileo Open Services and GPS modernized signals. The Sine BOC (further referred to as BOC) modulation splits the signal spectrum in two components, symmetrically placed around the carrier frequency, by multiplying the pseudorandom (PRN) code with a rectangular subcarrier [6]. The typical notation is BOC(f_{sc} , f_c) or BOC(m,n), with $m= f_{sc} / f_{ref}$ and $n= f_c / f_{ref}$, where f_c is the chip rate, f_{sc} is the sub-carrier frequency and f_{ref} is the reference frequency (generally f_{ref} =1.023 MHz). The resulting split-spectrum signal provides good frequency sharing, while offering simple implementation, good spectral efficiency, high accuracy, and enhanced multipath resolution [6]. The Power Spectral Density (PSD) of MBOC is a combination of BOC(1,1) spectrum and BOC(6,1) spectrum. One method of generating the MBOC spectrum is that of using Composite BOC (CBOC) time waveforms. The CBOC method is based on a weighted sum (or difference) of BOC(1,1) and BOC(6,1)-modulated code symbols [9]. In this paper we will use the CBOC(minus) modulation, defined as [8]:

$$s_{CBOC(-)}(t) = w_1 s_{BOC(1,1)}(t) - w_2 s_{BOC(6,1)}(t)$$
$$w_1 = \sqrt{10/11} \qquad w_2 = \sqrt{1/11} \qquad (1)$$

After passing through the RF front end and the intermediate frequency blocks, the received GNSS signal, downconverted and sampled, is fed to the baseband stages of the receiver. Here, the code tracking loop tracks the phase of the PRN code of the incoming signal. This loop employs a Delay Lock Loop (DLL) which calculates the correlation between the input signal and three replicas of the locally generated code. The three replicas (Early,

ISBN: 978-1-61804-138-8

Prompt and Late) are produced with an equal spacing between them. The replica that presents the highest correlation characterizes best the delay between the prompt replica and the received code.

One of the most popular code tracking algorithm is called Early-Minus-Late (EML). It uses a 0.5 chip spacing between the three local replicas. Because of the large spacing, the EML method does not require important processing resources, but, in the same time, it has limited multipath mitigation capability. The correlation lobes of the multipath replicas of the received signal can be falsely identified by the algorithm as the main correlation lobe of the received signal and, thus, positioning errors can occur. Therefore, several optimized EML-based techniques have been introduced, especially to mitigate closely spaced multipath signals [10]. One type of these enhanced EML methods, referred to as narrow EML (nEML) is based on the idea of strongly reducing the 1 chip spacing between the early and late correlators [11].

4 Filtering techniques

The first two filtering methods employed in our research eliminate the CWIs by using an infinite impulse response notch filter, explained in [12]. It is a second order filter and its Z domain transfer function $H_N(z)$ is represented by the next equation:

$$H_N(z) = \frac{1+\alpha}{2} \cdot \frac{1-2\beta z^{-1}+z^{-2}}{1-\beta(1+\alpha)z^{-1}+\alpha z^{-2}} \quad (2)$$

Parameters α and β are defined as:

$$\alpha = \frac{1-\tan(\beta/2)}{1+\tan(\beta/2)} \qquad \beta = \cos(\omega_N), \omega_N \in [0,\pi] \quad (3)$$

where ω_N is the angular notch frequency, defined as $\omega_N = 2\pi f_c$, with f_c being the central frequency of the attenuating band of the filter. Parameter α controls the width of the -3 dB bandwidth and is fixed at α =0.989 for a minimum attenuation of the useful navigation signal. Parameter β tunes the central frequency of the notch filter.

The block diagram in Fig. 1 shows the behavior of the first filtering method, called the minimum power method. This is a time domain method, which uses a relative low amount of computational resources and no Fourier transformations. The detection technique employed by this method, represented by the blocks with red colored margins in the diagram, is based on a loop that executes itself as long as CWIs are detected. The detection takes place in the following manner:

- the central frequency of the filter is moved over all the spectrum of the input signal, by giving to β successive values that cover the interval (0,1);
- for each value of β, the same baseband sequence of the input signal is filtered by the notch filter and, thus, numerous output signals are obtained;
- the mean power of the output signals is computed and stored, obtaining a plot like the one presented in Fig. 2;
- as it can be seen in the example illustrated by Fig. 2, the mean power is mostly constant over the values of β, with the exception of several clear local minimums; they are caused by the CWIs, because the power of the output signal decreases visibly when the central frequency of the filter coincides with the frequency of the CWI and the power of the CWI (present at other values of β) is eliminated from the output power;
- the absolute minimum of the output power is located; it corresponds to a specific value of β and of the central frequency of the filter;
- if this minimum power is smaller than a threshold dependant on the overall mean power of the output signal, the detection of a CWI is declared, located at the frequency mentioned before; the authors have chosen the fixed proportionality factor between the mean power and the threshold after numerous trials, in order to obtain the best results;
- this CWI is eliminated by the notch filter from the input signal and the detection loop starts again, to look for other CWIs;
- the detection stage ends when no more CWIs are detected.

The actual filtering takes place after the detection. The notch filter is applied sequentially to the input signal, using the central frequencies found and stored during detection. After this filtering is over, the spectrum of the CBOC signal does not present any more CWIs, as it can be seen in the example plotted in Fig. 3. In the upper half of this figure, three CWIs have been added to the CBOC signal (the number of Dirac impulses is double in the figure because of the symmetry between the

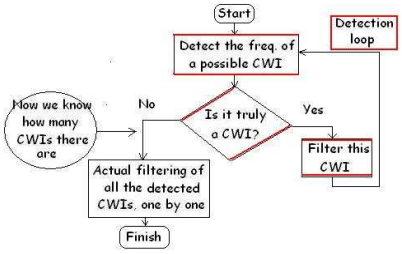

Fig. 1 Block diagram of the minimum power method

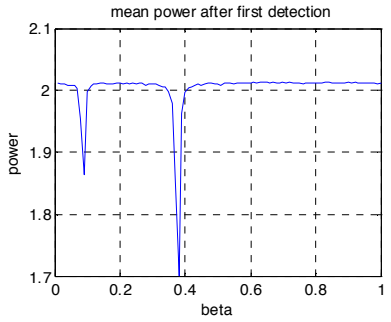

Fig. 2 Mean power of output signals vs. β

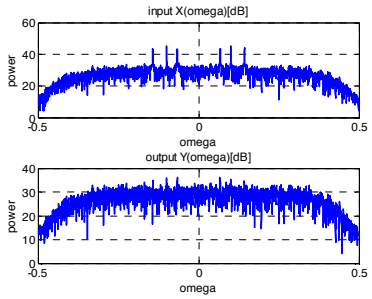

Fig. 3 Signal spectrum vs. angular frequency ω

negative and positive frequencies). After the detection and filtering stages are finished, the spectrum of the signal is free of interferences, as it is shown in the lower half of the figure.

The second filtering method used in this research detects the CWIs by exploiting the cyclostationarity property of the CBOC modulated signal. Signals that possess cyclostationarity present correlations between widely separated spectral components. The Spectral Correlation Function (SCF) is a function that illustrates this property. One benefit of cyclostationary approaches such as this is that Additive White Gaussian Noise (AWGN) is eliminated in these functions [16]. Thus SCF surpasses Power Spectral Density (PSD) detectors in reduced Signal to Noise Ratio (SNR) conditions. Cyclostationary processes are processes whose statistical parameters, namely mean value and autocorrelation function (ACF), show periodicity [17]. The SCF shows how much the spectral components of a process are correlated with other spectral components of the process. If the autocorrelation of a process is periodic with the period T_0, it shows that the autocorrelation has its own frequency, referred to as cycle frequency α. The cycle frequency can be defined as $\alpha = m/T_0$, where m is an integer [18].

In order to detect the CWIs, we use the information provided by the two dimensional matrix obtained from the SCF of the CBOC signal. The axes of this matrix are represented by α and the frequency f of the signal's spectrum. We extracted a row and a column from the matrix, obtaining two separate sources for the detection. The row corresponding to $\alpha=0$ is utilized in the 'frequency' version of the detection algorithm, and the column corresponding to $f=0$ produces the 'alpha' version of the detection. Both arrays are processed in the same way: the local maxima are located and their positions are stored, because they coincide with the frequencies of the CWIs. The reason for this is that the CWIs modify the periodicity of the mean values and of the ACF of the GNSS signal, and thus appear spikes in the SCF. Next, the stored frequencies are used in the actual filtering stage, to position the central frequency of the notch filter described earlier over the CWIs and to eliminate them one by one, like in the first method. This method requires more processing resources than the first one, because of the SCF.

The third filtering method used in our comparison is the zeroing method. As this method uses Fast Fourier Transform (FFT) and Inverse FFT (IFFT), it also produces a large computational load. It is a quite straightforward approach and it is explained next:

- initially a FFT is applied on the baseband sequence of the input signal and thus its spectrum is obtained.
- the absolute value of each sample of the spectrum is compared against a predefined threshold and if it is larger, it is considered to be a Dirac impulse and consequently a CWI; the authors have chosen the fixed proportionality factor between the mean value of the samples and the threshold after numerous trials, in order to obtain the best results;
- the CWIs are eliminated by changing the values of the samples that are higher than the threshold; the values become zero in the first version (named 'true zeroing') of this algorithm; in the second version (named 'mean zeroing'), they are given a predefined value, depending on the mean value of all the samples and thus the introduction of large amplitude variations in the spectrum of the GNSS signal is avoided;
- after checking the whole spectrum of the signal, an IFFT is applied to the filtered signal, to return it in the time domain.

5 Simulation setup

To analyze the effect of CWI, we have simulated via Matlab the tracking of a CBOC signal affected by

ISBN: 978-1-61804-138-8

interference in various degrees. The block diagram in Fig. 4 shows the main components of the simulation setup. The previously described CBOC signal (with f_c=1.023 MHz) is passed through a radio channel modeled with AWGN. The CWI is modeled by a single-frequency, continuous sine wave, which is summed with the CBOC signal. As a result, a Dirac impulse is added over each of the two main lobes of the CBOC spectrum. We simulated two scenarios, one with a single CWI, and another one with three simultaneous CWIs. Next, the resulting signal is fed to the filtering block. Afterwards, the filtered signal is processed by the tracking block, that employs the nEML algorithm.

The end result is represented by the curves of the Root Mean Square tracking Error versus SIR at several values of the C, for the five filtering methods explained earlier (minimum power, SCF frequency, SCF alpha, mean zeroing, true zeroing). Also the situation with no filtering is analyzed as a benchmark. The performances of these methods are examined by comparing the behavior of the RMSE as the value of SIR decreases.

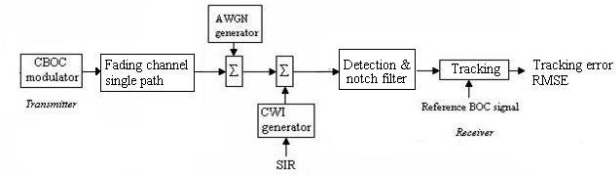

Fig. 4 Block diagram of the simulation setup

Parameter	Value
Channel model	uncorrelated, Nakagami-m=0.8
Number of paths	1
Oversampling factor	4
Coh. integration time	4 ms
Noncoh. integration time	1 ms
Initial delay error	0 chips

Table 1 Values of the simulation parameters

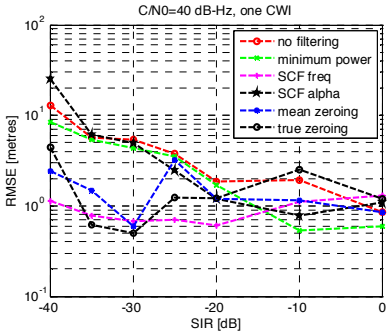

Fig. 5 Tracking RMSE vs. SIR for one CWI, at C/N_0=40 dB-Hz

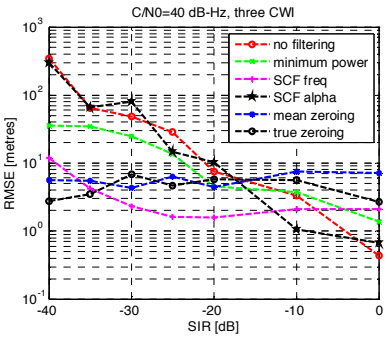

Fig. 6 Tracking RMSE vs. SIR for three CWIs, at C/N_0=40 dB-Hz

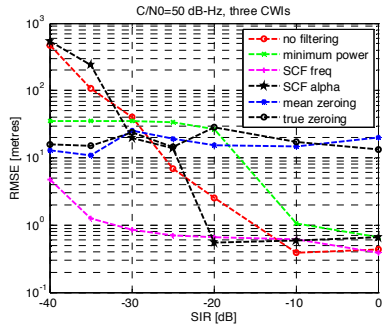

Fig. 7 Tracking RMSE vs. SIR for three CWIs, at C/N_0=50 dB-Hz

The simulation parameters are given in Table 1. SIR for one CWI is defined as:

$$SIR_{dB} = 20\log_{10}(\frac{1}{A_s}) \quad (4)$$

where A_s is the amplitude of the sine (absolute value) and the amplitude of the CBOC waveform is normalized to 1.

6 Simulation results

Extended simulations were run for a SIR covering the [-40, 0] dB interval, with a C/N_0 of 40 and 50 dB-Hz. Lower values of the C/N_0 provided unsatisfactory results for the RMSE.

For the first scenario, we generated one CWI. The resulting plot is illustrated in Fig. 5. This shows that the minimum power and SCF alpha methods outperform the no filtering case over most of the SIR interval.

In the second scenario, we generated three CWIs, each with the same power, and added them over each of the main lobes of the CBOC spectrum. The three CWIs are spaced at 0.5 MHz. Figures 6 and 7 present the resulting variations of RMSE over the SIR interval. It can be observed that the lowest error at high SIR is obtained through the minimum

ISBN: 978-1-61804-138-8

power and SCF alpha methods, but also without filtering. All the methods show more robustness to interference at low SIR (less than -20 dB) than the no filtering case.

7 Conclusions

In this paper, we propose an innovative approach, because we address the particular issue of filtering the CWIs affecting CBOC Galileo navigation signal, using several adaptive filtering techniques. To study the effectiveness of each method, we compare the tracking RMSE curves versus SIRs, at different C/N_0s.

In all the scenarios, both zeroing methods produce an almost constant tracking error, which is not correlated with the SIR increase. Thus, these algorithms are more suitable for situations with low SIR values. The best overall performance comes from the minimum power method, which does not need large processing resources. The SCF frequency method shows the best performance at low SIR. For further studies, the following topics seem to be interesting: optimization of the behaviour of the SCF frequency method at high SIR; evaluation of the effect of more than 3 CWIs on the RMSE.

Acknowledgment

This work has been supported partly by the grant PN II Parteneriate 92-100/2008, 2008-2011, by Nokia Foundation Visiting Professor Grant, by the Academy of Finland, and by the Spanish Government project TEC2011-28219, which are gratefully acknowledged.

References:

[1] The European GNSS (Galileo) Open Service *Signal in Space Interface Control Document*, Issue 1.1, September 2010.

[2] E. D. Kaplan and C.J. Hegarthy, *Understanding GPS Principles and application*, Artech House, Boston, 2006, pp. 244-247.

[3] Civil Aviation Authority of the United Kingdom, CAA PAPER 2003/9 *GPS Integrity and Potential Impact on Aviation Safety*, April 2004.

[4] A. Steingass, A. Hornbostel, H. Denks, Airborne measurements of DME interferers at the European hotspot, DLR, in Proceedings of *ENC GNSS,* Naples, Italy, May 2009.

[5] F. Klinker and O.B.M. Pietersen, *Interference of GPS signals: Influence of Licensed Transmitters on the GPS Signal Quality in the Netherlands' Airspace*, National Aerospace Laboratory NLR, May 2000.

[6] J.W. Betz, The Offset Carrier Modulation for GPS Modernization, in Proc. of *ION Technical Meeting*, June 1999, pp. 639-648.

[7] E. S. Lohan, A. Lakhzouri and M. Renfors, Binary-Offset-Carrier Modulation Techniques With Application in Satellite Navigation Systems, *Wireless Communications & Mobile Computing*, Vol. 7, 2007, pp. 767-779.

[8] J. Avila Rodriguez et al., CBOC- An Implementation of MBOC, *First CNES Workshop on Galileo Signals and Signal Processing*, Touluse, France, October 2006

[7] C. Hegarty et al., Suppresion of Pulsed Interference thorugh Blanking, Proceedings of the *56th Annual Meeting of The Institute of Navigation,* San Diego, CA, USA, June 2000, pp. 399-408.

[10] M. Z. H. Bhuiyan, X. Hu, E.S Lohan, and M. Renfors, Multipath mitigation performance of multi correlator based code tracking algorithms in closed and open loop model, in Proc. of *European Wireless Conference*, May 2009, Aalborg, Denmak.

[11] A. J. V. Dierendonck, P. C. Fenton, and T. Ford, Theory and Performance of Narrow Correlator Spacing in a GPS Receiver, *Journal of The Institute of Navigation*, No. 39, Vol. 3, June 1992.

[12] Y.R. Chien, Y.C. Huang, D.N. Yang, and H.W. Tsao, A Novel Continuous Wave Interference Detectable Adaptive Notch Filter for GPS Receiver, *GLOBECOM*, Miami, USA, Dec 2010, pp.1-6.

[13] D. Borio, L. Camoriano, L. Lo Presti, Two-Pole and Multi-Pole Notch Filters: a Computationally Effective Solution for Interference Detection and Mitigation, *ITST*, June 2007, pp.1-6.

[14] J. Vartiainen, J. Lehtomaki, H. Saarnisaari, M. Juntti, Limits of detection for the consecutive mean excision algorithms, Proceedings of *CROWNCOM*, June 2010, pp.1-5.

[15] D. Borio, L. Camoriano, S. Savasta, S.; L. Lo Presti, Time-Frequency Excision for GNSS Applications, *IEEE Systems Journal*, Vol. 2, No.1, March 2008, pp.27-37.

[16] D. Cabric, S.M. Mishra, and R.W. Brodersen, Implementation issues in spectrum sensing for cognitive radios, in Proceedings of *Asilomar Conf.*, pp. 772- 776, Nov. 2004.

[17] J. Goerlich et al., Signal analysis using spectral correlation measurement, Proc. of *Instrumentation and Measurement Technology Conf.*, pp.1313-1318, May 1998

[18] M. Song, *Characterizing cyclostationary features of digital modulated signals with empirical measurements using spectral correlation function*, MSc Thesis, Air Force Institute of Technology, Ohio,USA, June 2011.